RAPID COMMUNICATIONS

PHYSICAL REVIEW E VOLUME 51, NUMBER 6 JUNE 1995

Anchoring strength of a lyotropic nematic liquid crystal

A. M. Ribas, L. R. Evangelista, A. J. Palangana, and E. A. Oliveira*

Departamento de Física, Universidade Estadual de Maringá, 5790 Avenida Colombo, Maringá-Pr-87020-900, Brazil

(Received 3 January 1995)

We determine the anchoring strength (W) for a lyotropic liquid crystal in the nematic calamitic phase. The sample holder is a microslide 200 μm thick (Vitro Dynamics) whose inner surfaces present some grooves introducing an easy axis. The technique used is based on the determination of the critical magnetic field for a Frederiks transition. The values obtained are $W\sim 10^{-3}$ erg/cm^2 and the extrapolation length $L\sim 6$ μm.

PACS number(s): 61.30.Gd, 64.70.Md

Surface effects are widely used to obtain uniform orientation of liquid crystal films either for physical investigations or technological applications. The main feature of the surface treatment is to produce an easy axis $\vec{n}_0$, along which the molecules tend to align [1,2]. In analogy to Mayer-Saupe theory, the form of the anisotropic surface energy proposed by Rapini and Papoular [3] is given by $F_s=-\frac{1}{2}W(\vec{n}_0\cdot\vec{n})^2$ where $\vec{n}$ is the director and W is the anchoring strength coefficient. For dimensional reasons the anchoring strength is characterized by the extrapolation length $L=K/W$, where K is a curvature elastic constant [4]. For a thermotropic liquid crystal, typical values of W are between 10^{-5} and 10^{-1} erg/cm^2 [5–9]. The values of W and L are dependent on the temperature and on the surface treatment.

The anchoring properties of lyotropic liquid crystals are not completely similar to the thermotropics. It has been reported that the director at the boundary surfaces can glide and align parallel to the magnetic field in a flat glass surface [10,11]. These results indicate that the anchoring can be very weak. The purpose of this work is to evaluate the anchoring strength of a nematic lyotropic liquid crystal in the calamitic nematic phase with glass boundary surfaces of microslide commonly used in scientific investigations. The lyotropic sample consists of potassium laurate (29.4 wt %), decanol (6.6 wt %) and water (64 wt %). The phase sequence, determined by optical and conoscopic observations, is isotropic (15 °C)→calamitic nematic (50 °C)→isotropic. The birefringence of the sample measured as a function of the temperature is presented in Fig. 1. The sample is introduced by flux in a microslide (200 μm thick, 2 mm wide, and about 2 cm long) commercially available from Vitro Dynamics. The inner surfaces of these microslides were examined in an interferential microscope and grooves were detected parallel to its length. The grooves are about 0.5 μm deep and 1800 μm apart almost periodically. In Fig. 2(a) a typical interferogram of such a surface is shown. The distortions in the interference fringes are more evident when compared to the fringes produced by a glass cover plate [Fig. 2(b)] commonly used in microscopy. Diffraction patterns can also be observed in a transmission geometry using a laser beam. The existence of the grooves breaks the symmetry at the surface and can be characterized as an easy direction which would favor the alignment of the director parallel to the length of the microslide.

The Fredericks transition has been used to determine the anchoring strength coefficient in many different experiments [12–14]. In a recent paper, this method has been applied to the determination of the bend elastic constant (K_3) and the anisotropy of magnetic susceptibility (χ_a) for lyotropic liquid crystals [15,16]. The same method will be used in this investigation. The experiment is performed at 25 ± 1 °C, which corresponds to the maximum of the birefringence. The laboratory frame axes are defined with the boundary surfaces parallel to the xy planes, at $z=d/2$ and $-d/2$ and the easy axis parallel to the x direction. We start with a nematic monodomain, with the director aligned parallel to the x axis. The uniform initial orientation is achieved by applying a strong magnetic field (~ 10 kG) parallel to the easy axis. Afterwards, the field along x is switched off and a fixed-strength-controlled magnetic field is applied along the y axis [15]. The director tends to orient either parallel or antiparallel to $\vec{H}$, if $\vec{H}$ is greater than a certain threshold field H_C. The two domains, parallel and antiparallel, are separated by a wall, and a periodic distortion of $\vec{n}$, with walls formed in the direction of $\vec{H}$, is observed in a polarized microscope. The wavelength of the periodic distortion is then directly measured as a function of the applied magnetic field. With this geometry we suppose that the components of the director can be expressed by

$$n_x=\cos\phi(x,z),$$
$$n_y=\sin\phi(x,z), \tag{1}$$
$$n_z=0,$$

where $\phi(x,z)$ is the angle between the director $\vec{n}$ and the easy axis direction. Assuming a finite anchoring energy at the surface and the easy axis parallel to x, the distortion free energy per unit length, along y, can be written as

$$f=\int_{-\infty}^{+\infty}dx\int_{-d/2}^{d/2}dz\ F(x,z)+\int_{-\infty}^{+\infty}\tfrac{1}{2}W_+\sin^2\phi(x,d/2)dx$$
$$+\int_{-\infty}^{+\infty}\tfrac{1}{2}W_-\sin^2\phi(x,-d/2)dx. \tag{2}$$

*Also at Instituto de Física, Universidade de São Paulo, P.O. Box 20516, São Paulo-SP, Brazil.

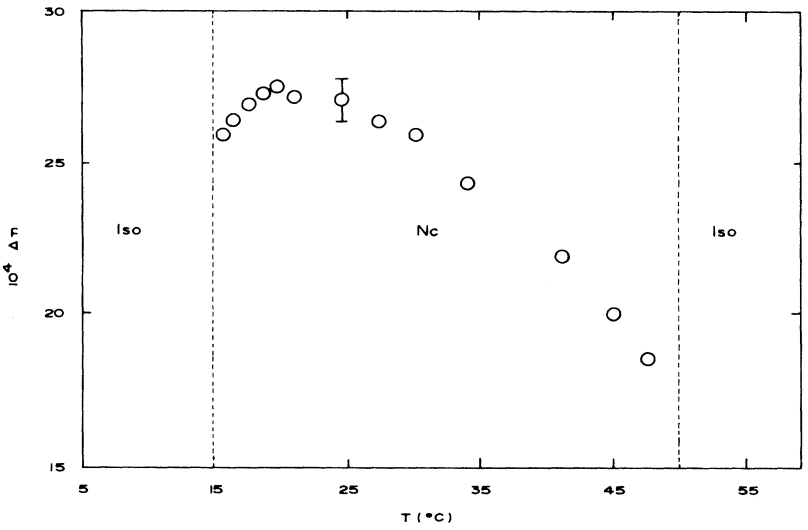

FIG. 1. Measured birefringence (Δn) as a function of the temperature for the lyotropic sample. Iso and N_C are, respectively, the isotropic and nematic calamitic phases. Typical error is shown in the figure.

In expression (2) $W_{\pm}$ refers to the anchoring strength at the upper (+) and lower (−) surfaces, and $F(x,z)$ is the bulk free-energy density, including the magnetic field coupling term, which is in the usual form written as [4]

$$F=\tfrac{1}{2}K_1(\vec{\nabla}\cdot\vec{n})^2+\tfrac{1}{2}K_2(\vec{n}\cdot\vec{\nabla}\times\vec{n})^2+\tfrac{1}{2}K_3(\vec{n}\times\vec{\nabla}\times\vec{n})^2 -\tfrac{1}{2}\chi_a(\vec{n}\cdot\vec{H})^2, \quad (3)$$

where K_1, K_2, and K_3 are, respectively, the elastic constants of splay, twist, and bend. The minimization of the free energy leads to the following differential equation:

$$\left[k_3\left(\frac{\partial\phi}{\partial x}\right)^2-\xi^{-2}\right]\sin\phi\cos\phi-[1+k_3\cos^2\phi]\frac{\partial^2\phi}{\partial x^2} -\frac{K_2}{K_1}\frac{\partial^2\phi}{\partial z^2}=0, \quad (4)$$

where $k_3=(K_3/K_1)-1$ and ξ is the magnetic coherence length defined by $\xi^2=K_1/(\chi_a H^2)$. With typical values of K_1, K_3, and χ_a for lyotropic liquid crystals [17,18] and with H in the range of 10^3 kG, the term $k_3(\partial\phi/\partial x)^2$ can be neglected when compared to ξ^{-2}. For small tilt angles Eq. (4) can be approximated

$$K_3\frac{\partial^2\phi}{\partial x^2}+K_2\frac{\partial^2\phi}{\partial z^2}+\chi_a H^2\phi=0. \quad (5)$$

The function $\phi(x,z)$ obtained from Eq. (5) must satisfy the boundary condition expressed by the following equation [19]:

$$K_2\left(\frac{\partial\phi}{\partial z}\right)_{z=d/2}+W\phi(x,d/2)=0. \quad (6)$$

Suppose that both boundary surfaces are identical ($W_+=W_-=W$), Eq. (6) can be easily solved by separating the variables, resulting in

$$\phi(x,z)=A\cos\left(\frac{2\pi x}{\lambda}+x_0\right)\cos(\theta z), \quad (7)$$

where λ represents the wavelength of the periodic distortion along the x axis, in such a way that $\phi(x,z)=\phi(x+\lambda,z)$. The solution of the differential equation holds only if λ obeys the following equation:

$$\lambda^{-2}=\frac{1}{4\pi^2}\left(\frac{\chi_a}{K_3}H^2-\frac{K_2}{K_3}\theta^2\right). \quad (8)$$

Equation (8) combined with the boundary conditions (6) implies that

$$\theta\frac{K_2}{W}=\cot\left(\theta\frac{d}{2}\right), \quad (9)$$

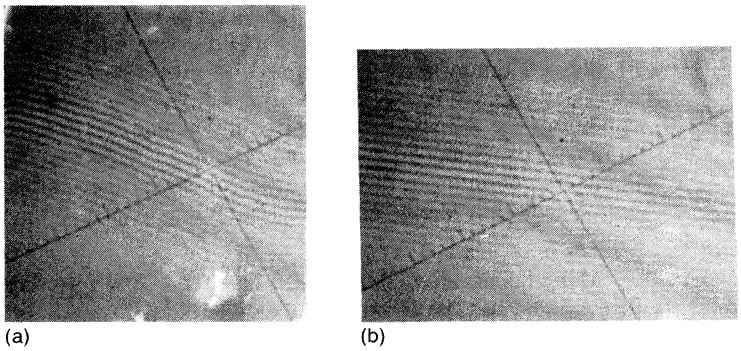

FIG. 2. Interference fringes for (a) microslides 200 μm thick and 2 mm wide, (b) glass cover plates used in microscopy.

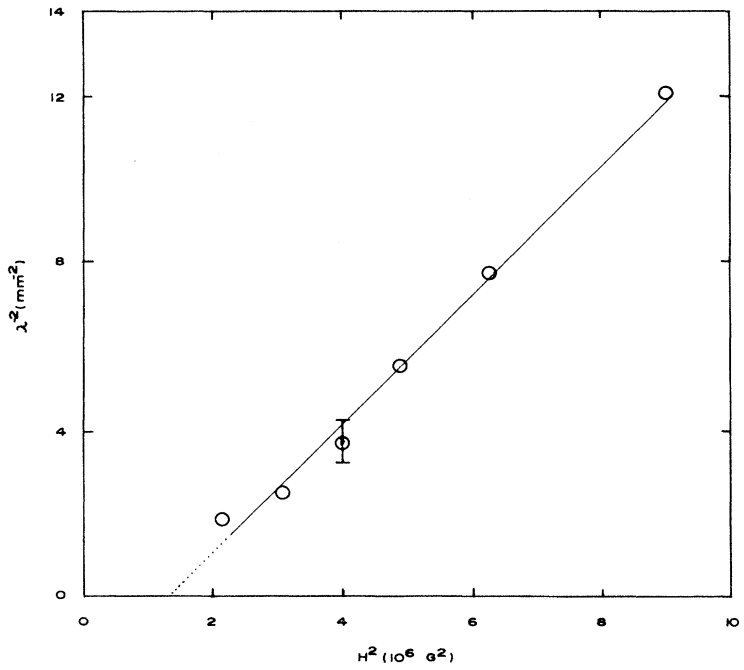

FIG. 3. Dependence of the wavelength of the periodic distortion λ on the applied magnetic field (H). The linear behavior is described by Eq. (8).

which, in the limit of the Frederiks threshold ($H \to H_C$ and $\lambda^{-2} \to 0$) reduces to the well known Rapini-Papoular expression [3],

$$L\sqrt{\frac{\chi_a H_C^2}{K_2}} = \cot\left(\sqrt{\frac{\chi_a H_C^2}{K_2}}\,\frac{d}{2}\right). \tag{10}$$

From Eq. (10) it is possible to determine the anchoring strength if the magnetic critical field and the physical constants involved are known. In Fig. 3 the experimental values of λ^{-2} are plotted as a function of H^{-2}. For low intensities of the magnetic field the approximation of small distortion is satisfied and the experimental points can be fitted by a straight line, given by Eq. (8). From the slope of the curve one obtains the ratio $K_s/\chi_a \cong 164$ dyn. Recent measurements are found in the literature for lyotropic systems resulting essentially in similar values for this ratio [20,21]. The value of the critical magnetic field obtained from the fitting is $H_C \cong 1.2\times 10^3 G$. If rigid boundary conditions were assumed the critical magnetic field calculated by the usual equation, $H_C^* = \pi/d(K/\chi_a)^{1/2}$, would result in $H_C^* \cong 2\times 10^3 G$. It is evident, from Fig. 3, that such a magnetic field can still distort the texture of the nematic liquid crystal. Indeed, it is expected that when the boundary conditions are no longer rigid the threshold magnetic field is lower than H_C^*.

The periodic distortion is sufficiently stable to perform several measurements, although it takes a long time to appear when the magnetic field is close to threshold. In the relaxation process the walls collapse to closed elliptical loops [4]. The ratio between the axes of the ellipse is related to the ratio of the curvature elastic constants K_3/K_2, which is found to be ~ 2.5. With these values in Eq. (8), we determine the extrapolation length, $L \cong 6$ μm, and the anchoring strength, $W = K_2/L \cong 10^{-3}$ erg/cm^2. The results obtained are in the range of the values reported in the literature for thermotropic liquid crystals [22]. To decide whether the anchoring is strong or weak, we must compare the surface energy to the bulk energy. The typical bulk energy U is due to the molecular iterations and is of the order of K/a, where a is an average molecular dimension. The wall-nematic interaction energy is $U_{WN} \cong Wa^2$. Thus the ratio between the bulk and the surface energy is given by [4]

$$\frac{U}{U_{WN}} \cong \frac{L}{a}. \tag{11}$$

When U_{WN} is comparable to U, the extrapolation length is of the same order of the molecular dimension and the anchoring is said to be strong. On the other hand, for a weak anchoring, the extrapolation length becomes much larger than the molecular dimensions; $L/a \gg 1$ because U_{WN} may be much lower than U.

For a lyotropic liquid crystal, the parameter a should be identified as the micellar dimension, which is about 10^2 Å [23] and we obtain 6×10^2. Therefore U is about 10^2 greater than U_{WN}. In this case, with a weak anchoring at the surface, the surface alignment can be disrupted by the magnetic field and the boundary thin layers can be oriented. It is important to remark that for thermotropic liquid crystals weak anchoring is required for applications in liquid crystal displays [9] but this condition is easily obtained. In this experiment the sample thickness is large, 200 μm, but even under these conditions we are able to determine the anchoring strength. In many experiments with lyotropic liquid crystals rigid boundary conditions are assumed (strong anchoring) and we notice that this is not a valid assumption even for thick samples.

Many thanks are due to A. M. Figueiredo Neto for useful discussions, and the Brazilian Agency (CNPq) for partial financial support.

[1] J. Cognard, Mol. Cryst. Liq. Cryst. Suppl. **1**, 1 (1982).
[2] B. Jerome, Rep. Prog. Phys. **54**, 391 (1991).
[3] A. Rapini and M. Papoular, J. Phys. (Paris) Colloq. **30**, C4-54 (1964).
[4] P. G. de Gennes, *The Physics of Liquid Crystals*, 2nd ed. (Clarendon, Oxford, 1993).
[5] G. Barbero, N. V. Madhusudana, J. F. Palierne, and G. Durand, Phys. Lett. **103A**, 385 (1984).
[6] G. Barbero, N. V. Madhusudana, and G. Durand, J. Phys. (Paris) Lett. **45**, L613 (1984).
[7] S. Faetti, M. Gatti, V. Palleschi, and T. J. Sluckin, Phys. Rev. Lett. **55**, 1681 (1985).
[8] K. H. Yang, J. Appl. Phys. **53**, 6742 (1982).
[9] R. Barberi and G. Durand, Phys. Rev. A **41**, 2207 (1990).
[10] E. A. Oliveira, A. M. Figueiredo Neto, and G. Durand, Phys. Rev. A **44**, 825 (1991).
[11] E. A. Oliveira and A. M. Figueiredo Neto, Phys. Rev. E **49**, 629 (1994).
[12] S. Naemura, J. Phys. (Paris) Colloq. **40**, C3-514 (1979).
[13] S. Naemura, J. Appl. Phys. **51**, 6149 (1989).
[14] C. Rosenblatt, Phys. Rev. Lett. **53**, 791 (1984).
[15] T. Kroin and A. M. Figueiredo Neto, Phys. Rev. A **36**, 2987 (1987).
[16] T. Kroin, A. J. Palangana, and A. M. Figueiredo Neto, Phys. Rev. A **39**, 5373 (1989).
[17] M. Stefanov and A. Saupe, Mol. Cryst. Liq. Cryst. **108**, 309 (1984).
[18] E. Zhou, M. Stefanov, and A. Saupe, J. Chem. Phys. **88**, 5137 (1988).
[19] G. Barbero and R. Barberi, *Physics of Liquid Crystalline Materials* (Gordon and Breach, Philadelphia, 1991).
[20] T. Kroin, Ph.D. thesis, Instituto de Física, Universidade de São Paulo, 1990 (unpublished).
[21] A. V. A Pinto and L. Q. Amaral, J. Phys. Chem. **94**, 3186 (1990).
[22] L. M. Blinov, A. Yu. Kabayenkov, and A. A. Sonin, Liq. Cryst. **5**, 645 (1989).
[23] Y. Galerne, A. M. Figueiredo Neto, and L. Liebert, J. Chem. Phys. **87**, 1851 (1987).

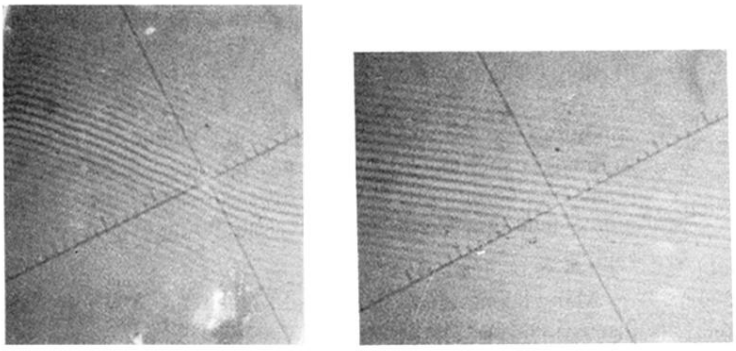

(a) (b)

FIG. 2. Interference fringes for (a) microslides 200 μm thick and 2 mm wide, (b) glass cover plates used in microscopy.